frontiers | Frontiers in Earth Science

ORIGINAL RESEARCH
published: 25 April 2022
doi: 10.3389/feart.2022.891319

Looking Into the Entanglement Between Karst Landforms and Fault Activity in Carbonate Ridges: The Fibreno Fault System (Central Italy)

Michele Saroli[1,2†], *Matteo Albano*[2*†], *Marco Moro*[2], *Emanuela Falcucci*[2], *Stefano Gori*[2], *Fabrizio Galadini*[2] *and Marco Petitta*[3]

[1]Università degli studi di Cassino e del Lazio Meridionale, Dipartimento di Ingegneria Civile e Meccanica, Cassino, Italy, [2]Istituto Nazionale di Geofisica e Vulcanologia, Roma, Italy, [3]Sapienza Università di Roma, Dipartimento di Scienze della Terra, Roma, Italy

The entanglement between active tectonics and karst systems is well-known in the literature. Karst systems are sound recorders of continental deformation in terms of brittle structures and seismic features and have been successfully used as markers for reconstructing tectonic stresses and assessing preferential directions of increased permeability in oil and gas fields. Karst systems could also be exploited to evaluate the past activity of faults bounding karst hydrostructures, thus providing useful data for the assessment of the seismic hazard of a specific area. In this work, we look into the complex relationship among karst development, recent tectonics and groundwater flow, which appear to be strongly interconnected with each other, to assess the activity of faults bounding karst hydrostructures. We focused our attention on an active karst area located in the Mesozoic and Cenozoic carbonate reliefs of the Italian central Apennines. In this context, the morphological and morphometric features of the karst landforms (dolines, dry valleys, and cave entrances), identified with geomorphological surveys, and their mutual relationship with fractures and fault segments, identified employing geostructural analysis, document stasis and deepening events in karst evolution. Such events are related to changes in the groundwater table and the consequent variation of the paleokarst base level associated with the Quaternary fault activity. A comprehensive evaluation of the evolution of karst systems at local and regional scales, considering the hydrogeological influence on base levels, allows us to use karst landforms as a proxy to unravel fault activity and evolution in Italy and in other similar karst environments.

Keywords: active faults, karst landforms, hydrogeology, tectonics, fibreno fault, seismic hazard

OPEN ACCESS

Edited by:
Alessandro Tibaldi,
University of Milano-Bicocca, Italy

Reviewed by:
Alberto Tazioli,
Marche Polytechnic University, Italy
Michele Lancia,
Southern University of Science and Technology, China

****Correspondence:***
Matteo Albano
matteo.albano@ingv.it

†These authors have contributed equally to this work and share first authorship

Specialty section:
This article was submitted to Structural Geology and Tectonics, a section of the journal Frontiers in Earth Science

Received: *07 March 2022*
Accepted: *04 April 2022*
Published: *25 April 2022*

Citation:
Saroli M, Albano M, Moro M, Falcucci E, Gori S, Galadini F and Petitta M (2022) Looking Into the Entanglement Between Karst Landforms and Fault Activity in Carbonate Ridges: The Fibreno Fault System (Central Italy). Front. Earth Sci. 10:891319. doi: 10.3389/feart.2022.891319

INTRODUCTION

The role of tectonics and the paleo stress field in the genesis of surficial and underground karst landforms has been largely established in the literature. Tectonic discontinuities, such as fractures and faults, control karst systems' spatial distribution and orientation and determine the mechanical limits of karst expansion (Thery et al., 1999; Shanov and Kostov, 2015; Öztürk et al., 2018).

It has been demonstrated in examples from different areas that karst systems are sound recorders of continental deformation in terms of brittle structures and seismic features (Shanov and Kostov, 2015 and references therein). Indeed, karst features, such as dolines and karst conduits, often occur

when two or more discontinuity systems converge, and the evolution of tectonic discontinuities favours their growth (Basso et al., 2013 and references therein). Once karst features are formed, their development, which frequently occurs through the formation of aggregate landforms by the coalescence of individual dolines, is still strongly governed by the tectonic evolution of the area (Bauer, 2015). Karst systems are also remodelled by vertical ground movements caused by tectonics and fault activity, which modify the relative position between permeable and impermeable layers and alter groundwater flow and water table level (Santangelo and Santo, 1991). Indeed, several case studies in the literature investigated the role of faults in groundwater circulation and testified to changes in groundwater flow regime after strong earthquakes, as in the case of 1980, November 23 (Irpinia and Basilicata, M_w 6.8) and 2016, October 30 (Norcia, M_w 6.5) events (Cotecchia et al., 1989; Gudmundsson, 2000; Bense et al., 2013; De Luca et al., 2018; Rosen et al., 2018; Ingebritsen and Manga, 2019; Mastrorillo et al., 2020; Fronzi et al., 2021).

The interaction between tectonics and karst systems has been successfully used as a marker for reconstructing tectonic stresses, assessing preferential directions of increased permeability in oil and gas fields, and estimating the geotechnical behaviour of the hosting rocks (Faivre and Reiffsteck, 1999; Karfakis and Loupasakis, 2006; Shanov and Kostov, 2015; Abdullah, 2021; Bagni et al., 2022). However, a further application has not been deeply assessed in the literature. Indeed, karst systems could also be exploited to evaluate the past activity of faults bounding karst hydrostructures. The purpose of this work is then to look into the complex relationships among karst development, recent tectonics and groundwater flow, which appear to be strongly interconnected such as to be considered entangled among them.

The reciprocity of these three geological processes is demonstrated here in a case study in Italy. Still, other geological and hydrogeological environments in tectonically active areas around the globe could be investigated when the following conditions are satisfied. In detail, 1) the karst hydrostructures must be hydraulically disconnected from each other, 2) they must be bounded by hydraulic barriers, often represented by permeability bounds or regional or local tectonic lineaments (i.e., a fault) with predominantly extensional kinematics, and 3) they must host a phreatic aquifer, mainly conveying groundwater to a preferential delivery area where several large springs occur, often at the border of the main faults. Together with relative or absolute chronological constraints on the involved lithologies, such conditions could allow assessing the tectonic activity of fault segments bordering karst hydrostructures and then providing valuable data for evaluating the seismic hazard of the area.

We focused our attention on the Mesozoic and Cenozoic carbonate reliefs of the Italian central Apennines. These represent a valuable case study since they constitute several regional natural groundwater reservoirs (e.g., Gran Sasso chain, Mt. Maiella, Mt. Morrone, Marsica Mts, Simbruini-Ernici-Cairo Mts, Lepini-Ausoni-Aurunci Mts, Venafro Mts, Meta-Mainarde Mts, Matese Mts, Alburni-Cervati Mts.) often characterised by a well-developed karst network and by several springs located at the boundaries of the aquifers (Celico, 1983; Boni et al., 1986; Capelli et al., 2012), thus meeting the conditions described above.

In particular, the south-eastern sector of the Western Marsica Mts. hydrostructure (**Figure 1A**) shows the most impressive karst features of the central Apennines (Saroli et al., 2003; Cipriani and Roncacè, 2020), such as dolines, polje, dry valleys and cave entrances. The structure is bounded by a regional fault, known in the literature as the "Val Roveto-Atina Line" (VAFS in **Figure 1A**). This fault places the Miocene and Cretaceous carbonate rocks in contact with the Early Miocene siliciclastic (clayey-arenaceous) flysch and the Quaternary deposits of the tectonic-karst depression hosting the *Fibreno* lake (**Figure 1A**). This depression, holding large karst springs, marks the contact between permeable and impermeable lithologies and currently identifies the hydrogeological and karst base level of the whole Western Marsica Mts. hydrostructure.

The performed geological, hydrogeological and geomorphological investigations allowed us to assess that the genesis of epigean and hypogean karst landforms in the investigated area is the result of the action of extensional tectonics, whose activity from the upper Pleistocene to Holocene times modified the spatial and temporal stability of the groundwater flow lines and influenced the karst system development. In this context, the Fibreno fault system (hereinafter FFS), a segment belonging to the VAFS, acted as the main kinematic dislocation in the last 2.6 Ma.

TECTONIC, GEOLOGICAL AND HYDROGEOLOGICAL SETTING

The study area belongs to the southern sector of the Western Marsica Mts (the area enclosed in the dashed black box in **Figure 1A**), corresponding to the *Terelle Hill* carbonate relief and encompassed among the *Pescosolido*, *Posta Fibreno, Vicalvi* and *Alvito* villages. This chain sector formed mainly during the Neogene period (Saroli et al., 2003 and references therein), when Meso-Cenozoic carbonate deposits and upper Miocene terrigenous sediments were intensively deformed by the eastward piggy-back propagation of a thrust sequence (Malinverno and Ryan, 1986; Patacca et al., 1990). In this framework, the Simbruini-Ernici thrust sheet (SET in **Figure 1A**), emplaced in the Messinian, was affected by out-of-sequence processes (Scrocca and Tozzi, 1999 and references therein). Several mountain belts developed due to orogenesis and the Apennines build-up, generating the Marsica Mts. domain (Cipollari et al., 1995).

Starting from the Late Miocene, extensional tectonics, associated with backarc rifting, dissected the Apennine chain with normal and oblique faults cutting through the pre-existing compressional structures (Doglioni et al., 1991; Carminati et al., 2012). These displaced the whole chain with a series of NW-SE trending normal faults, among which the Comino fault (CF in **Figure 1A**) and the Val Roveto-Atina Fault System (VAFS in **Figure 1A**) can be recognized in the study area. In particular, the latter is interpreted in the literature as a crustal fault reaching the

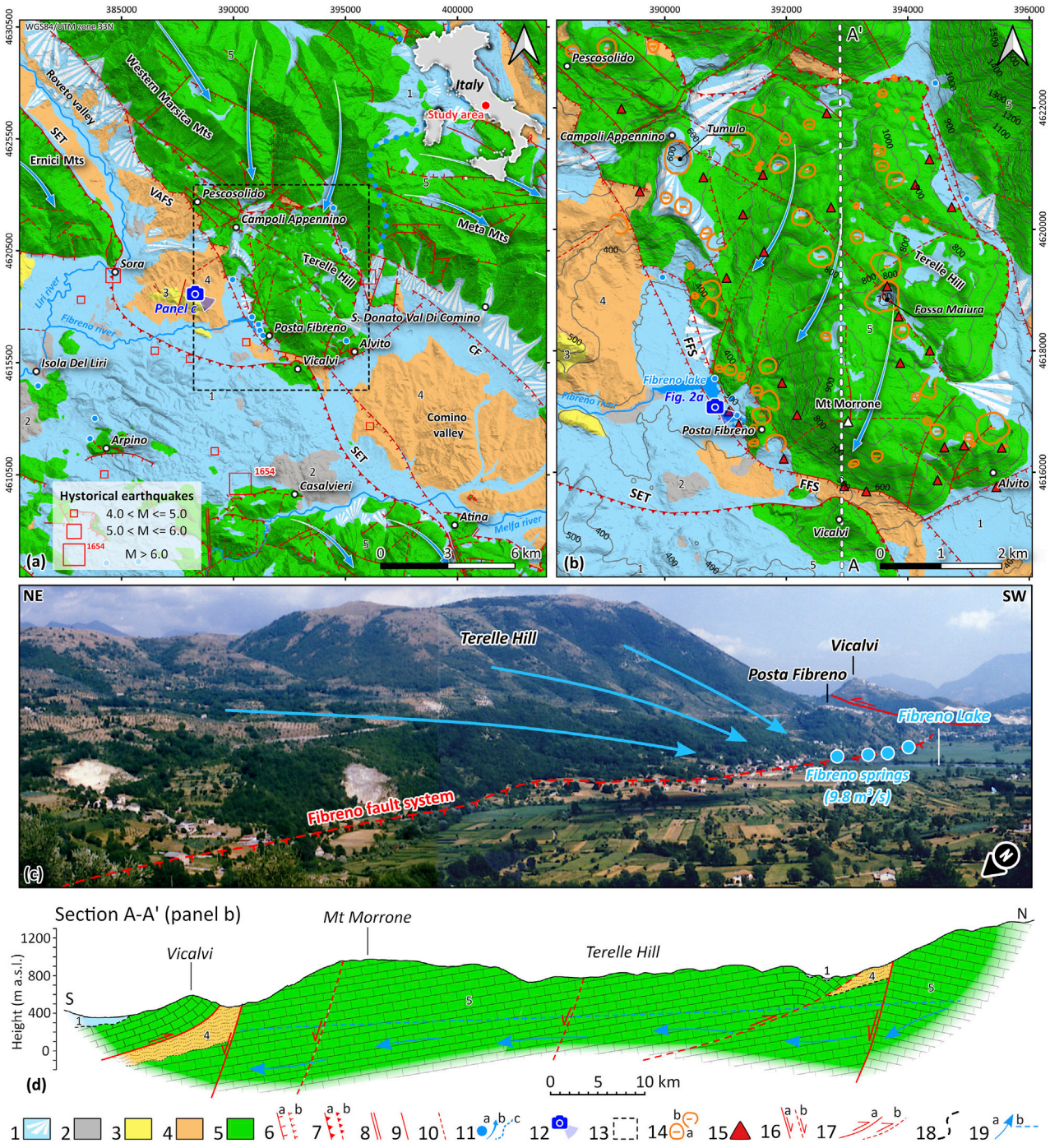

FIGURE 1 | Geological and hydrogeological sketch of the study area. **(A)** Overview of *Roveto* and *Comino* valleys (southern and northern sectors, respectively), showing main tectonic features and pre-Quaternary and Quaternary deposits, modified from Saroli et al. (2003). Historical earthquakes with magnitude M > 4 are taken from the parametric catalogue of Italian earthquakes (Rovida et al., 2021). The date of the main event which struck the investigated area has been reported in red. **(B)** Detail of the inset in panel A. **(C)** Panoramic view of the *Terelle Hill* area; the Fibreno fault (dashed red line), springs and *Fibreno* lake have been indicated. **(D)** Hydrogeological cross-section along the A-A′ profile in panel b, modified from Saroli et al. (2003). Key to the legend: 1) Recent and old debris, debris fan, eluvial, colluvial and lacustrine deposits (upper Pliocene - Holocene). 2) Travertine (middle Pleistocene - upper Pleistocene). 3) Gravel and sand (Messinian - lower Pliocene). 4) Sandstone and grey clay (flysch) (upper Tortonian). 5) limestone and dolostone with hemipelagic marl (Lias - lower Tortonian). 6) Normal fault: (a) certain, (b) inferred 7) Thrust fault: (a) certain, (b) inferred. 8) Strike-slip fault. 9) Faults with complex kinematics. 10) Inferred/buried fault. 11) (a) spring or group of springs, (b) groundwater flow, (c) groundwater divide. 12) Location and orientation of pictures. 13) Detail of the study area in panel b. 14) Doline: (a) closed, (b) open. 15) Location of the geomechanical surveys. 16) Normal fault (panel d): (a) certain, (b) inferred. 17) Thrust fault (panel d): (a) certain, (b) inferred. 18) Inferred lithological boundary (panel d). 19) (a) groundwater flow, (b) groundwater table (panel d).

Moho discontinuity (Tiberti et al., 2005), as testified by the upwelling of deep fluids with high CO_2 content (Ciotoli et al., 1993). The main effect of the rising of deep fluids in carbonate aquifers is the lowering of the calcite saturation index, which is usually reached along the groundwater flow path. This condition restarts the karst processes, with obvious consequences on the permeability and evolution of karst landforms (Salvati and Sasowsky, 2002; Barberio et al., 2021).

In this context emplaced the *Terelle Hill* structure (**Figure 1B**), which shows a typical NW-SE Apennine trend. It is delimited, to the NE, by an out-of-sequence thrust of the SET main thrust and, to the SW, by the Fibreno normal fault system (FFS in **Figure 1B**), the latter being a segment of the VAFS fault system in **Figure 1A**. The VAFS is a normal fault dipping SW, with a listric geometry (Mostardini and Merlini, 1986) and a small left-lateral movement (Cavinato and Sirna, 1988; Montone and Salvini, 1991, 1993).

The lithostratigraphic sequence of the area begins with Meso-Cenozoic dolomites and limestones of the Latium-Abruzzi carbonate platform (n°5 in **Figure 1**) outcropping on the mountain ridges bounding the Roveto and Comino Valleys. These valleys are filled with approximately 700 m of a terrigenous sequence of sandstones and clayey sandstones (upper Miocene) (n°4 in **Figure 1**), representing the onset and development of a foredeep basin during the Messinian period. Polygenic conglomerates (upper Messinian-lower Pliocene), outcrop to the SW of the Roveto Valley (n°3 in **Figure 1**) and testify the transition from marine sedimentation to a brackish continental environment (Cosentino et al., 2010 and references therein). Finally, alluvial fan, flood plain, talus debris and cross-bedded conglomerate sequences (upper Pliocene - Holocene) (n°1 in **Figure 1**), testify the transition to a fully developed continental sedimentary environment, with local massive lenses of travertine (n°2 in **Figure 1**).

The seismicity of the area is dominated by NW-SE oriented normal fault systems (e.g., Val Roveto-Atina Fault System, Fucino fault, Atina-S. Pietro Infine fault). These spread all over the central-southern Apennine chain and are responsible for medium-to-large magnitude seismic events. Historical and instrumental data show that strong earthquakes reaching grade 10 MCS (Mercalli, Cancani Sieberg; Rovida et al., 2021) affected the area, causing severe damages to the *Sora* and *Alvito* villages during the 1,349, 1,456, 1,654, 1,688 (*Sora*), 1,805 (*Sora*) and 1,915 earthquakes (Serafini and Vittori, 1988; Montone and Salvini, 1991, 1993). Indeed, the probabilistic seismic hazard in the area is among the highest in Italy, with peak ground accelerations (PGA) at the bedrock higher than 0.25 g (Stucchi et al., 2004). A regional significance is attributed to the VAFS fault system. The seismogenic potential of this structure is still debated in the literature. Serafini and Vittori (1988) observed neotectonic, strike-slip displacements within the Quaternary conglomeratic deposits of *Campoli Appennino*. Other authors identified lower Pleistocene deformed alluvial sediments (Carrara et al., 1995), in the central-southern section of the fault along the Roveto Valley. In the southernmost sector, corresponding to the FFS segments in **Figure 1B**, recent activity referable to the dislocation of upper Pleistocene-Holocene sediments has been identified close to the inhabited areas of *Pescosolido*, *Campoli Appennino* (Saroli et al., 2006) and *Posta Fibreno*. In particular, the largest known earthquake in the area, namely the catastrophic event of July 1654 (**Figure 1A**) ($M_w \cong 6.3$), which destroyed *Posta Fibreno* and nearby villages, has been attributed to the FFS segment (Saroli et al., 2012). Indeed, the macroseismic intensity (Rovida et al., 2021) associated with such event is primarily distributed in the hanging wall of the FFS. Further evidence is testified by the collapsed doline of *La Prece* (picture in **Figure 2A**, with its location in **Figure 1B**). This landform is placed along the western slope of the hill where *Posta Fibreno* village is located and appears to have formed in recent geological times (**Figures 2A,B**). Indeed, an historical high-relief depicting the village of *Posta* (nowadays *Posta Fibreno*), dating back to the first decade of 1,600 and located in the *Mazzenga* villa (Castrucci, 1863), shows a barely visible small depression at the approximate location of *La Prece* doline (**Figure 2C**). Therefore, it is believed that *La Prece* doline collapsed during the 1,654 event and assumed its current shape (Agrillo et al., 2004; Saroli et al., 2012).

The hydrogeological setting of the area is dominated by the carbonate karst aquifer of the Western Marsica hydrostructure (Boni et al., 1986). The boundaries of such hydrostructure formed during the structuration of the Apennine chain and its compartmentalisation in several hydrostructures (Saroli et al., 2003). It remained substantially unchanged from the lower Pleistocene onwards. The recharge area mainly consists of Mesozoic dolomitic limestones with high relative permeability (n°5 in **Figure 1**). Here, water infiltration is favoured by the numerous dolines and karst depressions distributed along the topographic surface (**Figure 1B**), reaching effective infiltration values exceeding 800 mm/year (Capelli et al., 2012). The groundwater final delivery point is represented by high-discharge basal springs located at the most topographically depressed area of *Fibreno* lake (**Figures 1B,C**), at an altitude of approximately 300 m above sea level. With a mean discharge rate up to 9.8 m^3/s (Capelli et al., 2012), these springs are among the largest spring groups in Italy thus far and feed the *Fibreno* lake from several submerged delivery points (**Figure 1**). Here, the highly permeable carbonate karst is in stratigraphic and tectonic contact with the less permeable terrigenous sequence (n°4 in **Figure 1**). The other hydrogeological complexes (n° 3, 2, and 1 in **Figure 1**) are heterogeneous, with impermeable horizons made of clay or clayey silts, alternating with medium-to-high permeability layers of coarse sands, gravels and travertine. These host local perched aquifers, often confined, which are continuously fed by lateral contact with the carbonate karst aquifer.

METHODS

To look into the geometrical and possibly causative relationship between fault activity and the developement and evolution of the karst system of the *Terelle Hill* area, we carried out a multistage investigation through geomorphological and geostructural *in-situ* surveys, together with photogeological, morphometric and spatial analysis of karst features with the aid of Geographical Information Systems (GIS).

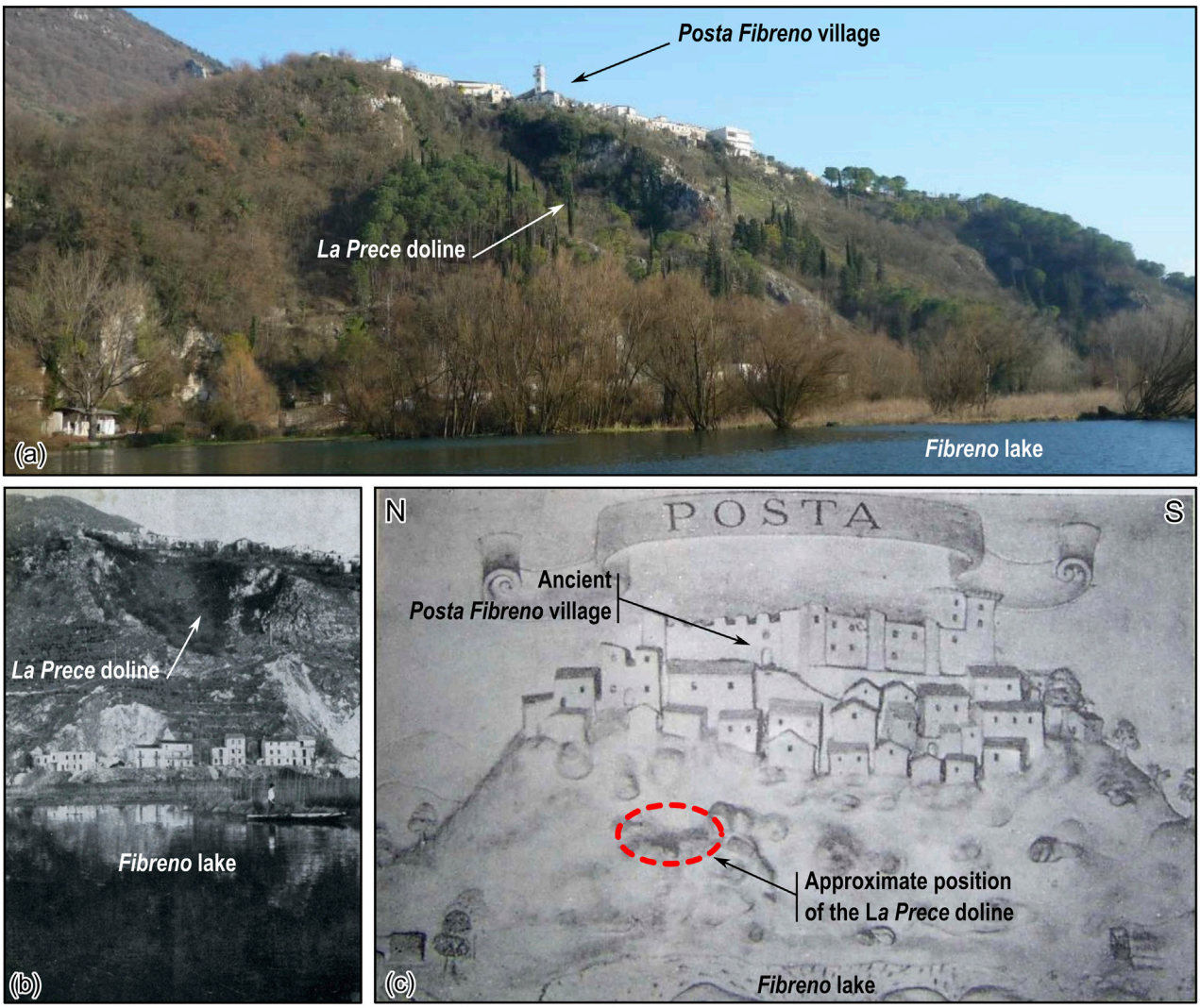

FIGURE 2 | (A) Present-day picture of the *La Prece* doline, taken from the *Fibreno* lake (for the location of the picture see **Figure 1B**) **(B)** Historical picture of *La Prece* collapsed doline, modified from Carbone (1965). **(C)** High relief dating back to the first decade of 1,600 and showing the ancient village *Posta* (nowadays *Posta Fibreno* in **Figure 1B**) seen from the *Fibreno* lake, located in the *Mazzenga* villa (Castrucci, 1863), modified from http://www.settefrati.net/enricaventurini/ducatodialvito/posta%20fibreno.jpg.

Since it is well-known that there is a close relationship between structural elements, such as faults and joint systems, and the orientation and density of landforms in karstic fields (Herold et al., 2000; Faivre and Reiffsteck, 2016; Öztürk et al., 2018), we firstly analysed the geometrical features of faults and discontinuities employing geostructural surveys. Then, we provided a photogeological and morphological analysis of karst features identified over the study area.

Geostructural Surveys

We performed *in-situ* geomechanical surveys to assess the main orientations of fractures and faults characterising the *Terelle Hill* carbonate massif. A total of 28 geomechanical survey stations and 100 measurements were made along the carbonate ridge at places where the bedrock is well exposed, without scree or vegetation cover (red triangles in **Figure 1B**). We identified and classified each rock mass discontinuity based on its main orientation, according to the principles of the geomechanical standards (ISRM, 1978).

Photogeological and Morphometric Analysis of Karst Features

Recognition and identification of karst features started from analysing the available 1:5,000 scale topographic maps, integrated with the interpretation of the available DEM and exploitation of multi-year aerial orthophotographs, the oldest dating back to the 1940s and 50s. Extensive fieldwork was carried out to check the features identified with GIS processing and map previously unrecognised karst landforms.

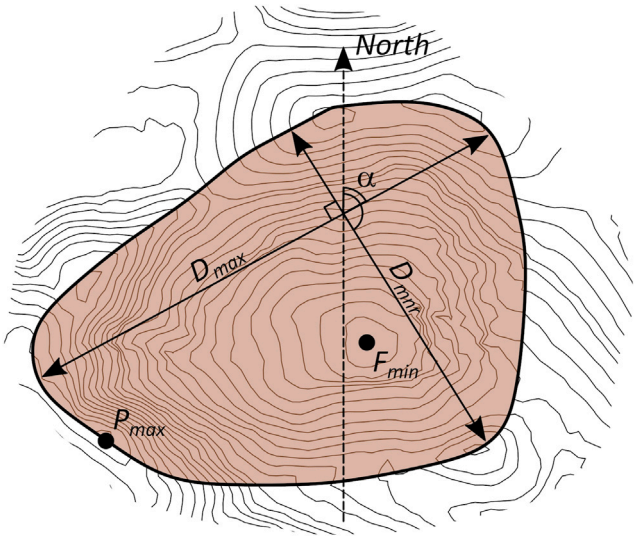

FIGURE 3 | Schematic representation of main morphometric parameters of dolines.

We classified karst forms such as dolines, polje, dry valleys and cave entrances with the available orthophotographs, a high-resolution TanDEM-X digital terrain model (DEM) (https://tandemx-science.dlr.de/), with relative vertical accuracy between 2 and 4 m and relative horizontal accuracy of 3 m, topographic maps, *in-situ* surveys, geological maps, and the available literature on the area (Saroli et al., 2003, 2015; Cipriani and Roncacè, 2020). Then, we performed a morphometric analysis on the identified karst features. Morphometric analysis is acknowledged as a useful tool to understand the evolution of karst systems, and it has been widely exploited to provide a quantitative description of morphometric features of karstic areas (Bondesan et al., 1992; Bruno et al., 2008; Basso et al., 2013; Bauer, 2015; Öztürk et al., 2018; Šegina et al., 2018; Verbovšek and Gabor, 2019; Pardo-Igúzquiza et al., 2020). A specially-devised GIS has been implemented, and several parameters have been calculated by developing ad-hoc algorithms in QGIS (QGIS Development Team, 2022).

The many morphometric parameters proposed in the scientific literature concerning doline classification were selected by choosing the most significant to describe the observed landforms (Bondesan et al., 1992). We initially identified dolines over the study area by visually inspecting the available topographic map, in conjunction with a hillshade visualisation of the available DEM. The dolines were first identified as point features (Bauer, 2015), defined by the deepest point of a single landform. Then, they were coded hierarchically according to 1) single doline with non-nested contours and 2) single doline with nested contours and lithology. We estimated the spatial distribution of the doline density *via* a Kernel Density function (KDE), calculating the density of the deepest point of dolines in a predefined neighbourhood around each feature. The search radius (SR) of the algorithm is estimated according to the following relation:

$$SR = 0.9 \times min\left(SD,\ \sqrt{1/ln(2)} \times D_m \right) \times n^{-0.2}$$

Where n is the number of available features, D_m is the weighted median of the distances between each feature point and the mean centre, and SD is the standard distance, given by:

$$SD = \sqrt{\frac{\sum_{i=1}^{n} w_i\left(x_i - \hat{X}_w\right)^2}{\sum_{i=1}^{n} w_i} + \frac{\sum_{i=1}^{n} w_i\left(y_i - \hat{Y}_w\right)^2}{\sum_{i=1}^{n} w_i} + \frac{\sum_{i=1}^{n} w_i\left(z_i - \hat{Z}_w\right)^2}{\sum_{i=1}^{n} w_i}}$$

Where x_i and y_i are the coordinates of the ith feature, w_i is the weight at feature i and $\{\widehat{X_w}, \widehat{Y_w}\}$ represent the weighted mean centre coordinates.

For the dolines characterised by closed boundaries, we identified the perimeter, defined as the closed line bounding the area morphologically influenced by the doline; the maximum diameter ($D_{\max}$ in **Figure 3**), i.e., the segment linking the two most distant points of the perimeter; and the minor diameter (D_{mnr} in **Figure 3**), defined as the longest segment connecting two points of the perimeter and perpendicular to the $D_{\max}$. Additionally, we measured the orientation angle to the north for both $D_{\max}$ and D_{mnr} (α in **Figure 3**). Other quantities were derived, such as the average diameter (D_{ave}), given by the arithmetical mean between $D_{\max}$ and D_{mnr}, and the elongation ratio (ER), i.e., the ratio between $D_{\max}$ and D_{mnr}.

$$D_{ave} = \frac{D_{max} + D_{mnr}}{2}$$

$$ER = \frac{D_{max}}{D_{mnr}}$$

Elevation parameters were determined from the available DEM. They comprised the minimum altitude of the doline bottom ($F_{\min}$ in **Figure 3**), defined as the elevation of the lowest point of the doline, the maximum altitude of the doline perimeter ($P_{\max}$ in **Figure 3**), and the maximum depth ($H_{\max}$), given by the difference in height between $P_{\max}$ and $F_{\min}$.

$$H_{max} = P_{max} - F_{min}$$

RESULTS

Geostructural Features of Faults and Discontinuities

In situ surveys identified three main discontinuities (**Figure 4A**) that belong to the FFS system (the FF, F1 and F2 in **Figure 4A**). Their identification is mainly inferred from the morphotectonic analysis since field evidence is often fragmentary and discontinuous. They show an orientation approximately NW-SE: the FF normal fault, bounding the *Fibreno* lake at an average height of roughly 290 m a.s.l.; the F1 normal fault at an average elevation of 400 m a.s.l.; and the F2 fault at approximately 650 m a.s.l. These segments represent the primary evidence of a complex system of normal faults displaying activity related to the Late Quaternary (Saroli et al., 2012). Evidence of FFS recent activity is testified by the displacement of plio-Quaternary continental conglomerates (n°1 in **Figure 4A** and pictures in **Figures**

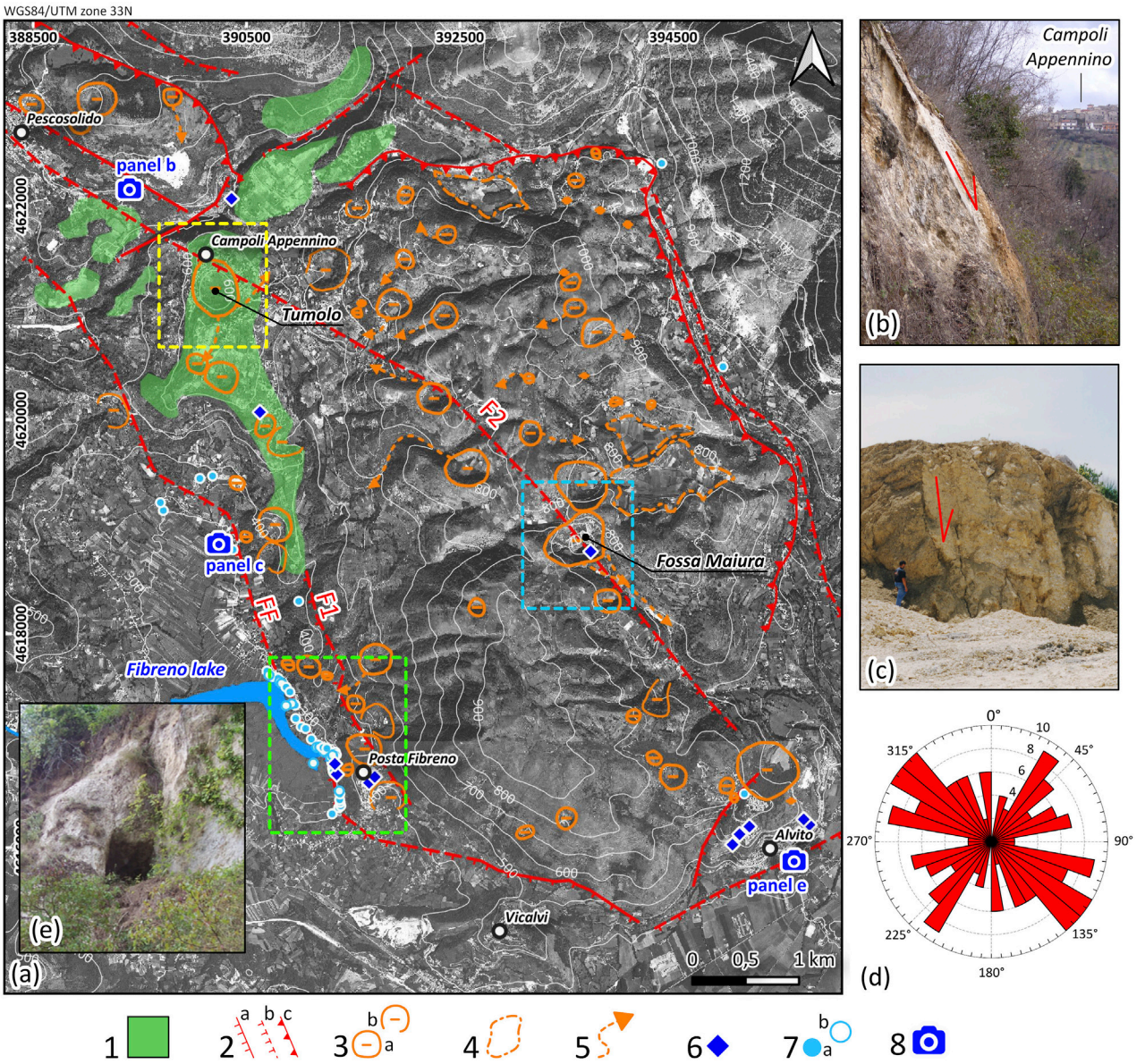

FIGURE 4 | Results of the geomorphological analyses performed over the study area. **(A)** Morphological map. **(B)** and **(C)** Evidence of dissection of upper Pleistocene–Holocene deposits by the FFS normal faults (FF, F1 and F2) in panel A; **(D)** Bidirectional rose diagram showing the observed fracture orientations at each geostructural station (bin size 10°). **(E)** example of a cave entrance. Key to the legend: 1) Plio-Quaternary continental conglomerates deposited approximately since 2.6 Ma (Saroli et al., 2015); 2) Main faults: (a) normal, (b) normal inferred, (c) thrust; 3) Dolines: (a) nested contours, (b) non-nested contours; 4) polje; 5) dry valley; 6) cave entrance; 7) Springs: (a) shoreline spring, (b) underwater spring; 8) Location of the pictures in panels b, c and e.

4B,C) (Saroli et al., 2015) and outcropping at different topographic elevations (Saroli et al., 2003). In detail, the outcrop in **Figure 4B**, located between *Pescosolido* and *Campoli Appennino*, shows a fault plane placing calcareous limestones in contact with displaced Holocene deposits made of colluvial gravels in a red matrix derived from colluvial paleosols. Carbon-14 dating of a bulk sample made of organic material indicated that Holocene deposits date back to approximately Cal. 4,600 to 4,450 BC (Saroli et al., 2006). The FF fault in **Figure 4C** dissects lacustrine sediments related to the *Fibreno* lake deposition during the upper Pleistocene-Holocene. Nowadays, this outcrop has been obliterated by quarry activities.

A synthesis of fractures distribution identified at the geostructural survey sites (red triangles in **Figure 1B**) is shown in the rose diagram in **Figure 4D**. We recognised five sets of discontinuities that identify two main orientations despite the dispersion of the retrieved dataset. The most frequent orientation develops along the NW-SE direction. It aligns perfectly with the normal faults belonging to the FFS system (i.e., the FF, F1 and F2 faults in **Figure 4A**) and, more generally, to the orientation of main faults in central Italy. The second group lines

up along the NE-SW direction. Both discontinuity sets mimic the overall geodynamics of the central Apennines, characterised by early compressive tectonics, accompanied by the development of thrust faults and strike-slip faults, and the later extensional tectonics associated with the growth of normal fault systems.

Morphological Analysis of Karst Features in the *Terelle Hill* Area

The study area (**Figure 4A**) is approximately 40.5 km^2, with altitudes varying between 290 m a.s.l (*Fibreno* lake) and 1,050 m a.s.l. Several karst features (**Figure 4A**) were identified, including polje, dolines, cave entrances, and abandoned valleys originating from the karst's rims. Dolines cover about 2% of the area, and their spatial distribution is not random (**Figure 5A**). Maximum doline density is found to be approximately five dolines/km^2 between the FF and F1 faults and in the north-easternmost part of the study area, where the doline density is probably ascribable to the large degree of fracturing of the carbonate relief caused by the anticline fold of the SET thrust fault (**Figure 1A**).

Dolines align approximately along the NW-SE direction, following the orientation of the main normal faults in the area, such as the FF, F1 and F2 segments in **Figure 5A**, thus suggesting that the structural setting has influenced karst development. Dolines spread all over the height interval of the site, i.e., between 290 and 1,050 m a.s.l (**Figure 5B**), but their distribution is not homogenous. Most of the dolines are located between 650 and 900 m a.s.l, with an additional doline concentration at approximately 300 m a.s.l, i.e., at the same height as the *Fibreno* lake and springs.

Concerning their shape, the computed elongation ratio (ER) in **Figure 5C** shows that sub-circular to elliptical shapes prevail (>80%). Less frequent, even though present, is the occurrence of the most typical circular shape for dolines (less than 4% in **Figure 5C**), which generally characterises all the small, developing features.

The rose diagrams of the D_{max} and D_{mnr} axes' orientation (**Figures 5D,E**) show that dolines are mostly elongated in the NW-SE direction. D_{max} perfectly aligns with the principal fracture orientation estimated from geomechanical surveys (**Figure 5D**), while the orientation of D_{mnr} agrees with the NE-SW subordinate fracture orientation as in **Figure 5E**. Such an aspect confirms the significant role of joint systems in the rock mass in governing the doline location in the area.

The computed average diameter (D_{ave} in **Figure 5F**) classifies the detected features as microdolines (≈5%), mesodolines (≈18%) and macrodolines (≈77%). The latter is the most frequent type, thus testifying that current karst processes likely began in the Early Quaternary. The long-term activity of karst processes is also testified by polje areas resulting from the coalescence of several dolines (**Figure 4A**).

A census of caves and karst conduits is not available in the study area. However, several cave entrances ascribable to small karst conduits have been recognised by *in-situ* surveys (blue diamonds in **Figure 4A** and the picture in **Figure 4E**). These are certainly not representative of the complex hypogean karst system of the area, but their altitude distribution, between 290 and 700 m a.s.l (**Figure 5B**), i.e., immediately below the maximum doline concentration (between 650 and 950 m a.s.l.), suggests that *Terelle Hill* is potentially pervaded by a well-developed network of karst conduits that convey the rainwater from the uppermost dolines to the lowermost spring system of the *Fibreno* lake. Such a hypothesis is corroborated by a particular historical event reported by Gerardo Canini in his book "I Forzati del Fibreno" (Canini, 2012), who tells that at the beginning of the last century, a gigantic walnut tree that was at the bottom of the *La Prece* doline, was uprooted by a violent storm and its trunk was swallowed by the great chasm that was created on the ground. After a few months, the same trunk came back to light, re-emerging from the *Fibreno* lake, thus testifying to the presence of an underground connection between *La Prece* doline and the lake itself.

Finally, abandoned dry valleys characterise a poorly developed hydrographic network. These dry valleys often originate from the rims of the dolines and seem to have no connection with the current hydrographic network.

DISCUSSION

The evolution of the *Terelle hill* karst system, with its dolines, polje, cave entrances, springs, and abandoned dry valleys, has been primarily conditioned by tectonics. An evident relationship exists between the detected structural elements, such as faults and joint systems (**Figure 4**), and the orientation and density of landforms. In particular, the epigean karst system, characterised by elliptical to sub-circular macrodolines (**Figure 5C**) approximately NW-SE oriented (D_{max} in **Figure 5D**), develops at different altitudes (**Figure 5B**) along approximately NW-SE oriented tectonic lineaments (**Figure 5A**). The latter corresponds to the primary orientation of fractures and joints in the area, as observed with *in-situ* geomechanical surveys (**Figure 4D**) and the direction of the VAFS line (**Figure 1**).

The *Terelle Hill* karst system also represents a significant example of karst processes acting at different temporal scales. Indeed, the identified karst landforms show various degrees of evolution. The *Fossa Maiura* and *Tumolo* macrodolines (**Figures 6**, **7**), with their morphological and morphometric features, and the dry valleys originating from the karst's rims, represent the oldest features of the area.

The *Fossa Maiura* doline (the noun "*Maiura*" means "the biggest"), with D_{max} = 588 m and H_{max} = 203 m, is the largest and deepest macrodoline in the area (**Figure 6A**). This landform is located approximately 3.5 km SE of *Campoli Appennino* village, in the middle of *Terelle Hill* (dashed blue rectangle in **Figure 4A**). It has an elliptical shape with a WNW-trending main axis and develops on Cretaceous limestones, dipping approximately 30° to more than 40°. Morphotectonic evidence shows that the carbonate bedrock is displaced by NW-SE-trending normal faults belonging to the FFS system (FF, F1 and F2 in **Figure 4A**), and it is pervasively fractured in the whole area. Its complex morphology, made of a funnel shape at the top and the bottom of the depression, and an intervening pit morphology,

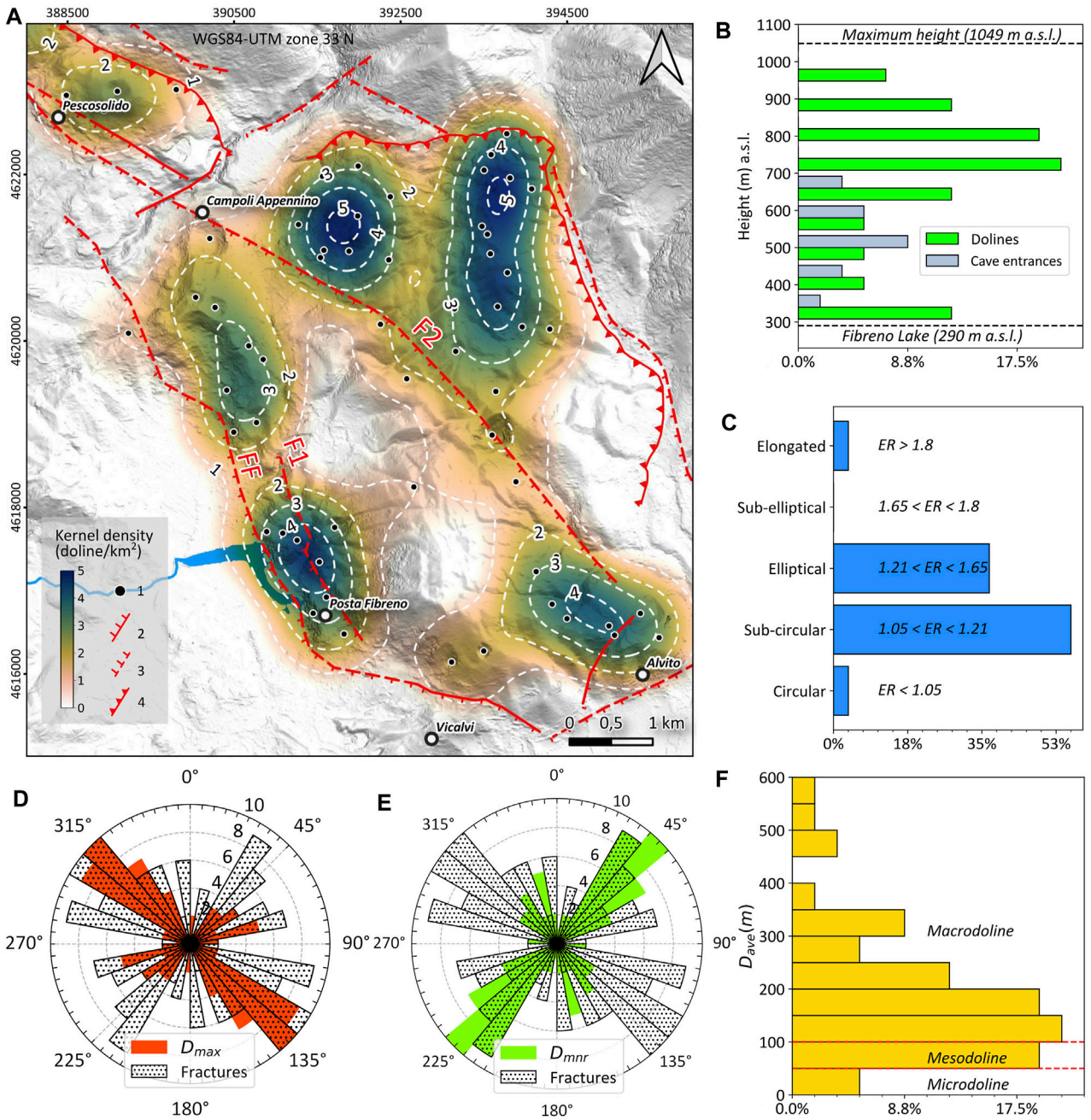

FIGURE 5 | Results of the performed morphometric analysis. **(A)** Kernel density distribution of the identified dolines. Key to the legend: 1) location of the deepest point of the doline; 2) Normal faults; 3) Inferred normal faults; 4) thrust faults. **(B)** altimetric distribution of dolines and cave entrances. **(C)** Doline classification according to the elongation ratio (ER). **(D)** and **(E)** Rose diagrams showing the orientation of maximum (D_{max} in panel d) and minor (D_{mnr} in panel e) doline diameter, together with the fracture orientations from geomechanical surveys **(Figure 4D)**. **(F)** Distribution of the average doline diameter (D_{ave}).

is probably the result of the coalescence of two concentric funnels. This configuration could testify to several karst erosive phases, forming a probable normal solution doline in the initial stage of karstification (funnel shape) and a collapse doline in the last stage (pit shape). The basal funnel morphology is related to the presence of residual deposits and scree sourced by gravity-related phenomena affecting the steep internal walls of the doline, which make the slopes smoother at the bottom (**Figures 6B,C**) (Cipriani and Roncacè, 2020 and references therein). The steep walls of the doline are affected by secondary karst forms such as epigean cave entrances (**Figure 6D**).

The *Tumolo* doline (**Figure 7A**; the dashed yellow rectangle in **Figure 4A**) presents an ovoidal shape roughly NE-SW

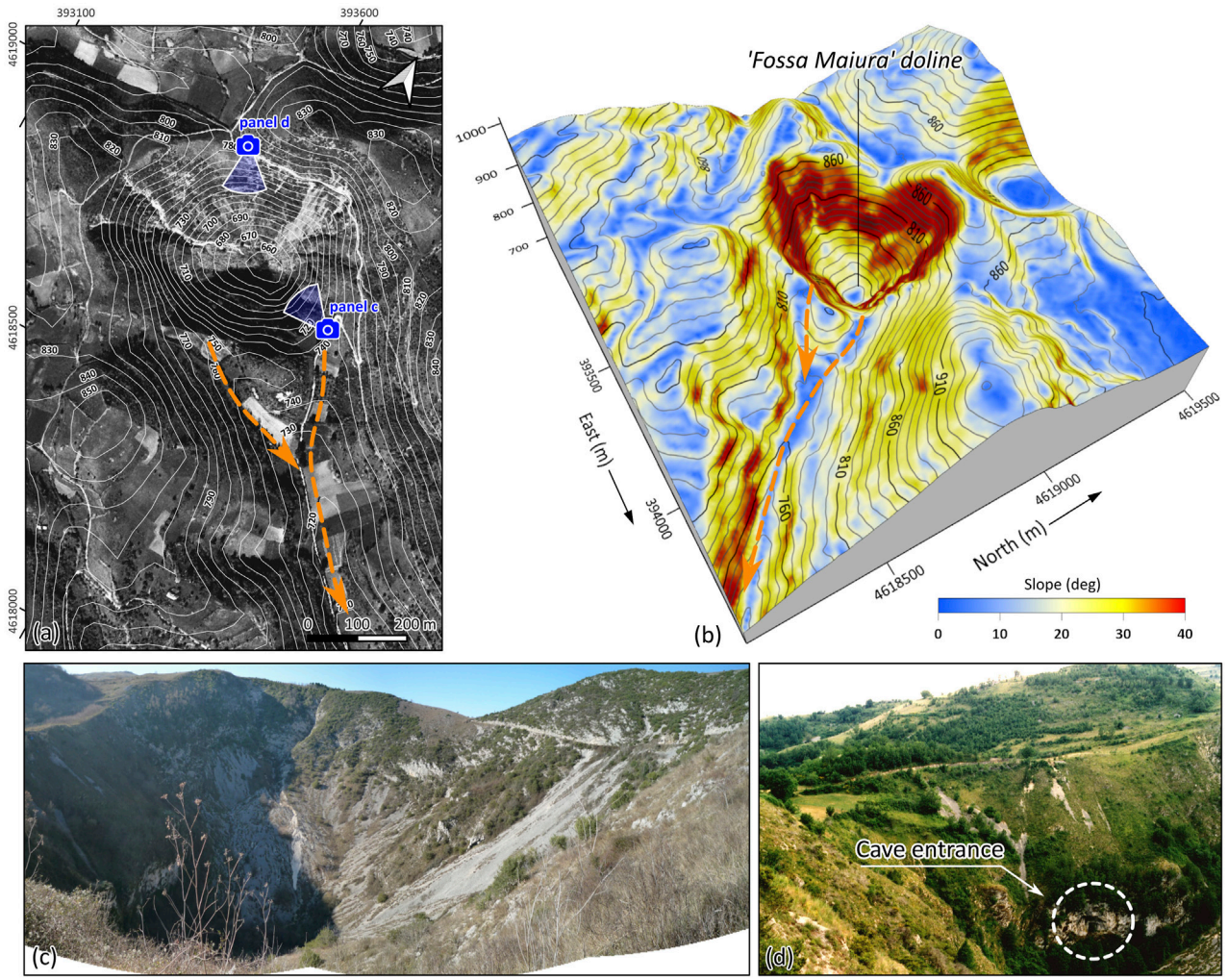

FIGURE 6 | *Fossa Maiura* doline (the dashed blue rectangle in **Figure 4A**). **(A)** Black and white orthophoto with the indication of dry valleys (the dashed orange arrows) **(B)** Three-dimensional sketch with the slope angle. **(C)** Panoramic view. **(D)** Indication of the cave entrance along the doline flank (the picture location and orientation are in panel a).

oriented with D_{max} = 546 m and H_{max} =123 m. The slopes are covered by a thick detrital blanket dipping approximately 20° and 35°, except for a small portion of the eastern flank where about 40 m-height cliffs made of Miocene limestones occur, dipping more than 40° (**Figure 7B**). Its peculiar shape and geographical position allowed for the development of the small settlement of *Campoli Appennino*, built along the whole doline rim (**Figure 7C**), and its exploitation as an agro-forestry-pastoral site from historical times to nowadays (Cipriani and Roncacè, 2020 and references therein). Unlike *Fossa Maiura*, the *Tumolo* doline developed from the dissolution of conglomeratic continental deposits called "*Campoli Appennino* conglomerates". The latter are made of heteromeric carbonate and arenaceous clasts dispersed in a sandy matrix and deposited approximately in the lower Pleistocene. Indeed, paleomagnetic measurements (Saroli et al., 2015) showed that the deposition of *Campoli Appennino* conglomerates occurred during the reverse Matuyama Chron, approximately between 2.581 and 0.781 Ma. Furthermore, based on analyses on the morpho-lithostratigraphic succession, Saroli et al. (2015) provided a narrower time interval for the deposition of the *Campoli Appennino* conglomerates, ranging approximately between 1.7 and 0.78 Ma. Therefore, the development of the *Tumolo* doline started in the same time interval. Being the *Tumolo* doline, together with *Fossa Maiura*, the oldest features of the area, we can argue that the onset of the karst processes in the area started between 1.7 and 0.78 Ma ago.

Both *Fossa Maiura and Tumolo* landforms present dry valleys starting from the rim of the dolines (dashed orange arrows in **Figures 6**, **7**). We interpreted such dry valleys as drainage paths that acted in the past when both dolines served as permanent or intermittent karst springs (i.e., estavellas) according to climate and groundwater conditions. Such dry valleys could also

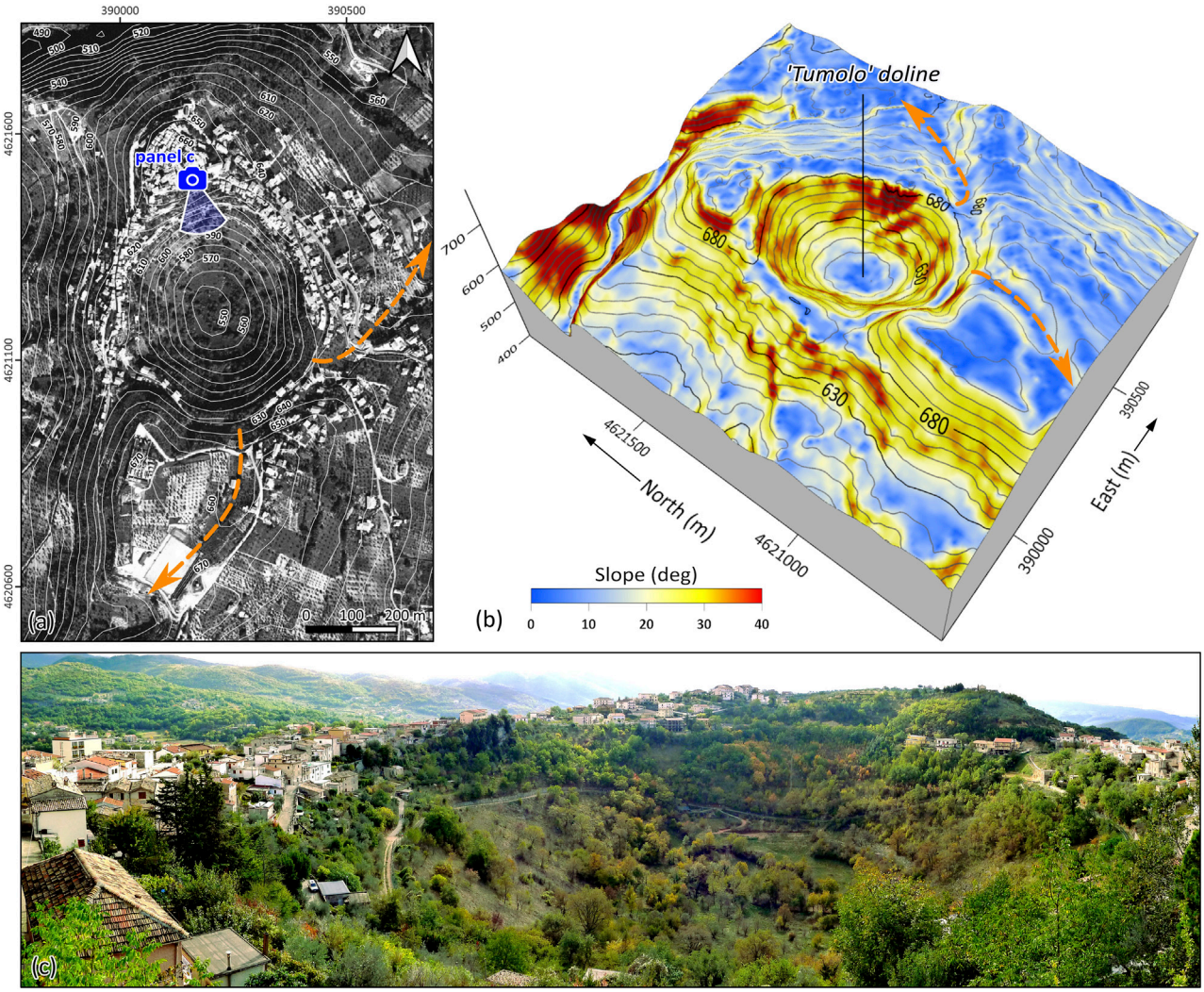

FIGURE 7 | *Tumolo* doline (the dashed yellow rectangle in **Figure 4A**). **(A)** Black and white orthophoto with the indication of dry valleys (the dashed orange arrows) **(B)** Three-dimensional sketch with the slope angle. **(C)** Panoramic view (the picture location and orientation are in panel a).

represent the relict system of a hydrographic network that formed before the doline development (Bočić et al., 2015). However, such a hypothesis is excluded since dry valleys start directly from the doline rim and do not show continuity of the paleo-drainage in the opposite part of the dolines.

On the other hand, the *Fibreno* lake area (**Figure 8A**, the dashed green rectangle in **Figure 4A**) shows evidence of active, short-term karst activity. In this area, the geomorphological and hydrogeological evolution of the lake basin has been controlled by Pleistocene-Holocene extensional tectonics (Saroli et al., 2003) and by the interaction between the Meso-Cenozoic carbonate bedrock, Miocene marly-arenaceous deposits, and deep fluids. Here, widespread epigean and hypogean karst processes act simultaneously (Nisio and Scapola, 2010; Cipriani, 2020), as evidenced by several dolines and dry valleys found northwest of the *Posta Fibreno* village (**Figure 8A**) and by many karst springs located inside submerged cavities, karst conduits and dolines along the shoreline and underwater (**Figure 8B**). These feed the *Fibreno* lake from the lake bottom or sideways through drainage paths as in **Figure 8B** (Agrillo et al., 2004) and align approximately along the inferred FF fault trace, where Meso-Cenozoic limestones and the Miocene marly-arenaceous deposits are in contact. Here, karstification processes are enhanced by the rise of CO_2-rich overpressured fluids that accelerate the chemical dissolution of calcium carbonate with the development of cavities and their subsequent collapse (Agrillo et al., 2004; Nisio and Scapola, 2010). Indeed, several recently formed chasms are present at the lake's bottom, often corresponding with submerged springs or spring groups (**Figure 8B**).

In such a contest, the morphology of *Fossa Maiura* and *Tumolo* dolines, with their ancient dry valleys and abandoned cave entrances (**Figures 6**, **7**), is surprisingly similar to the

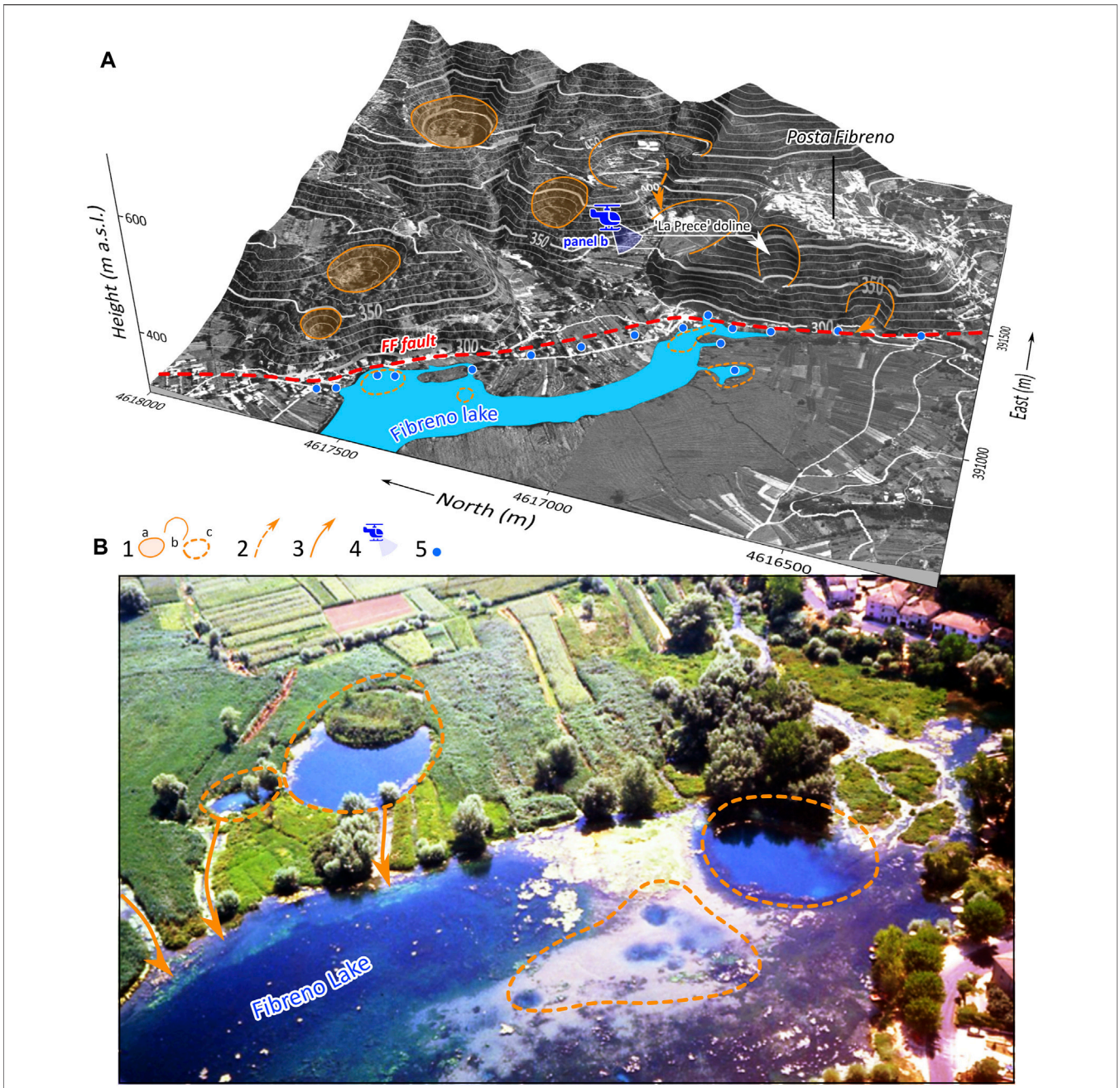

FIGURE 8 | (A) 3D view of the Fibreno lake area (the dashed green rectangle in **Figure 4A**), identifying dolines, springs and the *Fibreno* fault. **(B)** Helicopter view of part of the Fibreno lake, where hypogean karst processes are evident. Key to the legend: 1) Dolines or doline group (a) closed, (b) open, (c) submerged; 2) Dry valley. 3) Drainage path (panel b); 4) Location and orientation of the picture in panel b; 5) Springs.

submerged karst landforms and drainage paths located at the bottom of the basin in the active karst spring system of the *Fibreno* lake (**Figure 8B**). Such similarity can be interpreted according to the Quaternary structural evolution of the area, as shown in **Figure 9**. During the lower Pleistocene (t_0 in **Figure 9**), the hydrogeological setting of the *Terelle Hill* area was probably characterised by a primordial karst system constituted by karst springs, submerged karst conduits, and drainage paths similar to what is observed nowadays in the neoformations of the *Fibreno* lake.

Regional tectonic uplift associated with extensional tectonics and contemporary motion of the FFS extensional system modified the morpho-structural setting of the area (t_1 in **Figure 9**). The *Terelle Hill* progressively became a relief because of the coupled action of regional uplift and local fault activity. Due to tectonics, the submerged karst cavities and

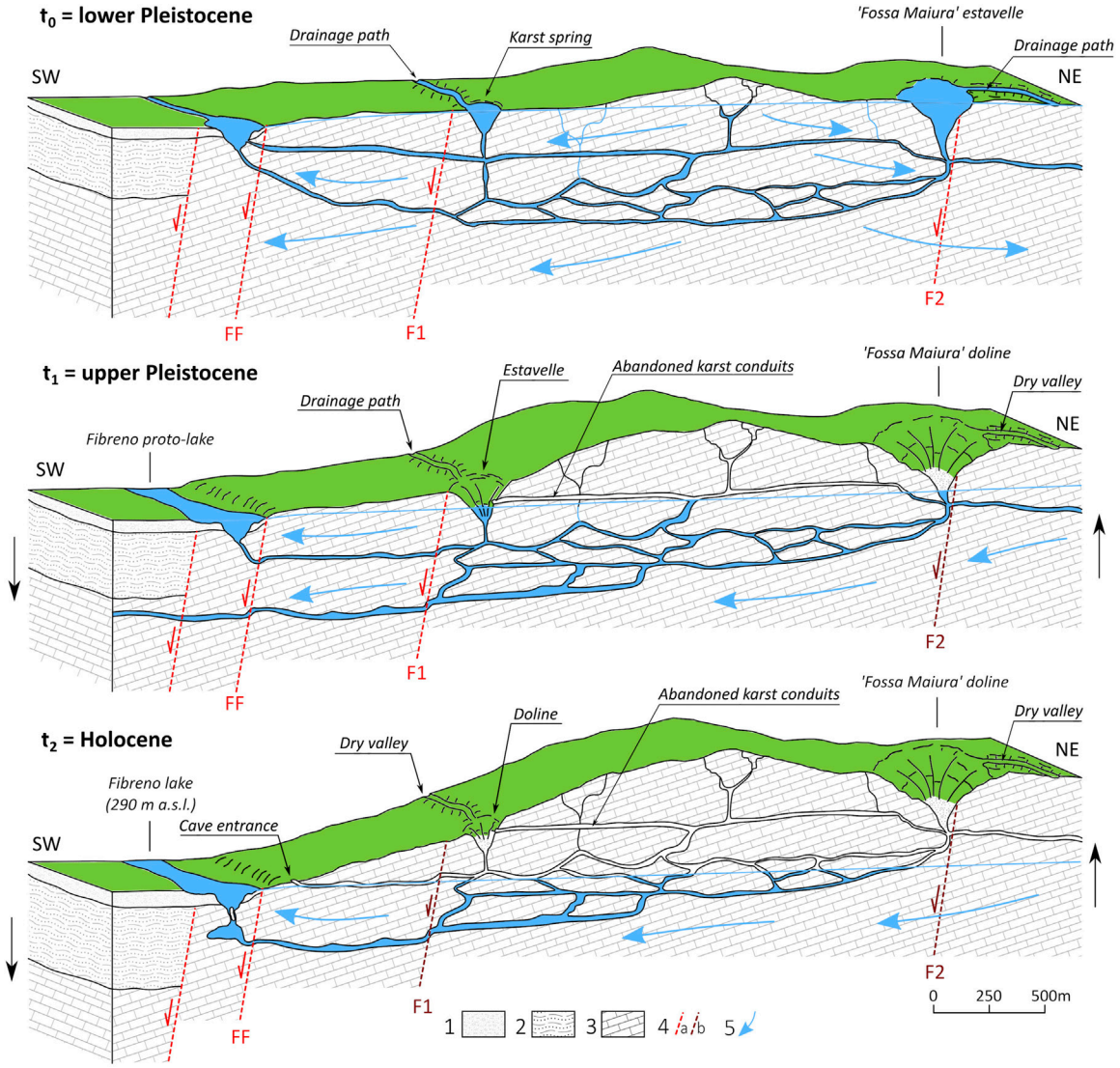

FIGURE 9 | Conceptual sketch of the model and evolution of the *Terelle Hill* karst system. Key to the legend: 1) Recent and old debris, debris fans, eluvial, colluvial and lacustrine soils (Pleistocene-Holocene). 2) Sandstones and grey clays (flysch) (Tortonian). 3) Limestones and dolostones with hemipelagic marls (Lias - lower Tortonian). 4) Active (a) and inactive (b) faults. 5) Groundwater flow. Caves and karst conduits are inferred.

dolines were raised at progressively increasing altitudes with respect to the groundwater table of the regional karst aquifer, thus evolving from karst springs to dolinesprings (estavelles). The karstic groundwater table was higher than what is observed nowadays, and probably it was highly variable. This means that, when the karstic water level was high, the water flowed out of the estavelles and supplied water to either a stream or a lake. Conversely, when the water table was low, the same karst crevice reabsorbed the water of the karst lake. This groundwater table's low- and high stages can be correlated with seasonal changes and long-term climate variability.

The identified epigean karst landforms, dolines, dry valleys, and cave entrances at different altitudes (**Figure 5**) testify to the progressive deepening of the local phreatic level, with the consequent variation of the basal level of karst development. In particular, the abandoned dry valleys of *Tumolo* and *Fossa Maiura* dolines (**Figures 6**, **7**), which start directly from the rims of the dolines, do not represent fluvial channels fed by meteoric water. Instead, they represent the ancient drainage paths of paleo-topographically higher springs of the Western Marsica hydrostructure, progressively depleted by the downthrowing of the *Fibreno* plain and the lowering of the hydrogeological base-flow level.

Following the continuous lifting of the *Terelle Hill* structure and the relative lowering of the groundwater base level (t_2 in **Figure 9**), the estavelles evolved into dolines. At the same time, the karst springs gradually lowered and migrated towards SW until reaching their current position at Fibreno lake.

It must also be noted that the active springs and estavelles in the *Fibreno* lake area are located only in the hanging wall of the

FFS, suggesting that deepening and migration of the karst system have not been spatially random with respect to the fault trace, as to indicate an influence of fault movements in the evolution of the karst system.

In this framework, the difference in altitude of approximately 500 m between the most elevated "paleo-springs" of *Fossa Maiura* and *Tumolo* (approximately 800 and 700 m a.s.l, respectively) and the current hydrogeological basal level of the Western Marsica hydrostructure, represented by the Fibreno lake springs (approximately 290 m a.s.l.), provides an approximate value of the cumulated vertical movement associated with the activity of the FFS fault system. Considering that the estimated onset of karst processes is comprised between 1.7 and 0.78 Ma ago (i.e., lower Pleistocene), this yields a displacement rate in the range of approximately 0.4–0.7 mm/yr associated with the FFS fault system. Such slip rates agree with the mean displacement rates of active faults in Italy, provided by paleoseismological analyses (Galadini and Galli, 2000; Galli et al., 2008).

CONCLUSION

The genesis of epigean and hypogean karst landforms in the paradigmatic study area of *Terelle Hill* is due to the simultaneous action of 1) extensional tectonics, which controlled the topographic elevation of the main freshwater springs, and 2) the stability, both in space and time, of the flow paths of the large karst aquifer of the Western Marsica Mts, which conveys groundwater to the main springs of the *Fibreno* lake.

Based on the performed geological, hydrogeological and geomorphological investigations, we were able to assess the onset of karst processes dating back to the lower Pleistocene. During the lifting of the structure, which used the southernmost section of the VAFS, i.e., the FFS system, as the main kinematic dislocation, the ancient karst springs gradually evolved in estavelles and then in dolines. Following the continuous lifting of the hydrostructure and the relative lowering of the karst base level owing to fault motion, the springs gradually lowered until they reached the current position at *Fibreno* lake.

In this framework, the difference in altitude between the current base level of the springs of the *Fibreno* lake and the higher paleo-springs (represented by the doline-dry valleys system of *Tumolo* and *Fossa Maiura*) provides an approximate value of vertical movement associated with the activity of the FF fault and the associated fault system (F1 and F2). The resulting displacement rate, given by the ratio between the vertical movement and the estimated onset of the karst process, would be in the range of 0.4–0.7 mm/year, as a function of the relative age of Quaternary sediments provided by the paleomagnetic method and the morpho-lithostratigraphic analyses carried out to date. Such displacement rate is associated with the FFS only but is not representative of the whole VAFS. The FFS represents a small portion of the VAFS; therefore, further analyses are required to assess the seismogenic potential of the entire structure.

The entanglement of the three investigated factors (karst development, tectonic activity and groundwater flow) results in a renovating process that can impact the prevision and the assessment of several geological risks, including earthquakes, groundwater resources vulnerability and management, slope stability and finally, water quality. The comprehension of the relationship among the three above-cited factors can surely help the researchers and decision-makers establish priorities in risk management in all areas where active tectonic coexists with anthropogenic activities (high population density, leading to water withdrawals and presence of human infrastructures).

DATA AVAILABILITY STATEMENT

The raw data supporting the conclusions of this article will be made available by the authors, without undue reservation.

AUTHOR CONTRIBUTIONS

MS and MA, contributed to conception and design of the study. MS, MM, EF, and SG performed the *in-situ* surveys and organised the database. MA performed the statistical and spatial analysis. MA wrote the first draft of the manuscript. MS, FG, and MP wrote sections of the manuscript. All authors contributed to manuscript revision, read, and approved the submitted version.

ACKNOWLEDGMENTS

We thank the German Aerospace Center for providing the TanDEM-X digital terrain model. Figures are made with the freely available codes, QGIS v.3.22 (https://www.qgis.org/it/site/), Matplotlib v.3.5 (https://matplotlib.org/) and Inkscape v.1.1.1 (https://inkscape.org).

REFERENCES

Abdullah, F. H. (2021). Porosity and Permeability of Karst Carbonate Rocks along an Unconformity Outcrop: A Case Study from the Upper Dammam Formation Exposure in Kuwait, Arabian Gulf. *Heliyon* 7, e07444. doi:10.1016/J.HELIYON.2021.E07444

Agrillo, E., Bono, P., Casella, L., D'Andrea, L., and Caramanna, G. (2004). "Cavità di collasso recenti e antiche nel bacino lacustre di Posta Fibreno (Frosinone)," in *Stato dell'arte sullo studio dei fenomeni di sinkholes e ruolo delle amministrazioni statali e locali nel governo del territorio* (Roma), 709.

Bagni, F. L., Erthal, M. M., Tonietto, S. N., Maia, R. P., Bezerra, F. H., Balsamo, F., et al. (2022). Karstified Layers and Caves Formed by Superposed Epigenic Dissolution along Subaerial Unconformities in Carbonate Rocks - Impact on Reservoir-Scale Permeability. *Mar. Pet. Geology.* 138, 105523. doi:10.1016/J.MARPETGEO.2022.105523

Barberio, M. D., Gori, F., Barbieri, M., Boschetti, T., Caracausi, A., Cardello, G. L., et al. (2021). Understanding the Origin and Mixing of Deep Fluids in Shallow Aquifers and Possible Implications for Crustal Deformation Studies: San

Vittorino Plain, Central Apennines. *Appl. Sci.* 202111, 1353. doi:10.3390/APP11041353

Basso, A., Bruno, E., Parise, M., and Pepe, M. (2013). Morphometric Analysis of Sinkholes in a Karst Coastal Area of Southern Apulia (Italy). *Environ. Earth Sci.* 70, 2545–2559. doi:10.1007/s12665-013-2297-z

Bauer, C. (2015). Analysis of Dolines Using Multiple Methods Applied to Airborne Laser Scanning Data. *Geomorphology* 250, 78–88. doi:10.1016/j.geomorph.2015.08.015

Bense, V. F., Gleeson, T., Loveless, S. E., Bour, O., and Scibek, J. (2013). Fault Zone Hydrogeology. *Earth-Science Rev.* 127, 171–192. doi:10.1016/j.earscirev.2013.09.008

Bočić, N., Pahernik, M., and Mihevc, A. (2015). Geomorphological Significance of the Palaeodrainage Network on a Karst Plateau: The Una-Korana Plateau, Dinaric Karst, Croatia. *Geomorphology* 247, 55–65. doi:10.1016/J.GEOMORPH.2015.01.028

Bondesan, A., Meneghel, M., and Sauro, U. (1992). Morphometric Analysis of Dolines. *Ijs* 21, 1–55. doi:10.5038/1827-806X.21.1.1

Boni, C. F., Bono, P., and Capelli, G. (1986). Schema Idrogeologico dell'Italia Centrale. *Mem. Della Soc. Geol. Ital.* 35, 991–1012.

Bruno, E., Calcaterra, D., and Parise, M. (2008). Development and Morphometry of Sinkholes in Coastal plains of Apulia, Southern Italy. Preliminary Sinkhole Susceptibility Assessment. *Eng. Geology.* 99, 198–209. doi:10.1016/j.enggeo.2007.11.017

Canini, G. (2012). I Forzati Del Fibreno (Ovvero Del Tempo in Cui Il Signore Della Palude Imponeva Sacrifici Umani). Lulu.com Available at: https://www.amazon.it/Forzati-Fibreno-Signore-Imponeva-Sacrifici/dp/1471722902 (Accessed March 3, 2022).

Capelli, G., Mastrorillo, L., Mazza, R., Petitta, M., Baldoni, T., Banzato, F., et al. (2012). *Carta idrogeologica del territorio della Regione Lazio, scala 1:100000*. Firenze: Regione Lazio - S.EL.CA.

Carbone, A. (1965). Vicalvi, Posta Fibreno, Il Fibreno. Tipografia dell'Abbazia di Casamari Available at: https://books.google.it/books?id=HHdMGwAACAAJ.

Carminati, E., Lustrino, M., and Doglioni, C. (2012). Geodynamic Evolution of the central and Western Mediterranean: Tectonics vs. Igneous Petrology Constraints. *Tectonophysics* 579, 173–192. doi:10.1016/j.tecto.2012.01.026

Carrara, C., Dai Pra, G., and Giraudi, C. (1995). "Lineamenti di tettonica plio-quaternaria dell'area," in *Lazio Meridionale, Sintesi Delle Ricerche Geologiche Multidisciplinari* (Roma: ENEA Dipartimento Ambiente), 151–155.

Castrucci, P. M. (1863). *Descrizione del Ducato d'Alvito nel Regno di Napoli*. 4th ed. Napoli: Stamperia Piscopo.

Cavinato, G. P., and Sirna, M. (1988). Elementi di tettonica transpressiva lungo la linea di Atina (Lazio meridionale)*Mem. della Soc. Geol. Ital.* 41, 1179–1190.

Celico, P. (1983). Idrogeologia dei massicci carbonatici, delle piane quaternarie e delle aree vulcaniche dell'Italia centromeridionale (Marche, Lazio meridionale, Abruzzo, Molise e Campania). *Quad. Della Cassa per Mezzog* 4, 1–203.

Ciotoli, G., Etiope, G., Lombardi, S., Naso, G., and Tallini, M. (1993). Geological and Soil-Gas Investigations for Tectonic Prospecting: Preliminary Results over the Val Roveto Fault (central Italy). *Geol. Rom.* XXIX, 483–493.

Cipollari, P., Cosentino, D., and Parotto, M. (1995). "Modello Cinematico-Strutturale dell'Italia Centrale," in *Studi Geologici Camerti* (Camerino: Università di Camerino), 135–143. doi:10.15165/studgeocam-927

Cipriani, A. (2020). Il Lago di Posta Fibreno (FR). *Mem. Descr. Della Cart. Geol. D'italia* 106, 165–176.

Cipriani, A., and Roncacè, S. (2020). The Dolines of Campoli Appennino (Frosinone, Italy): a Geo-Historical Overview. *Rol* 52, 77–102. doi:10.3301/ROL.2020.16

Cosentino, D., Cipollari, P., Marsili, P., and Scrocca, D. (2010). Geology of the central Apennines: a Regional Review. *J.Virt.Ex* 36. doi:10.3809/jvirtex.2010.00223

Cotecchia, V., Salvemini, A., and Ventrella, N. A. (1989). Interpretazione degli abbassamenti territoriali indotti dal terremoto del 23 Novembre 1908 e correlazioni con i danni osservati su talune strutture ingegneristiche dell'area epicentrale irpina. *Riv. Ital. di Geotec.* 4, 145.

De Luca, G., Di Carlo, G., and Tallini, M. (20182018). A Record of Changes in the Gran Sasso Groundwater before, during and after the 2016 Amatrice Earthquake, central Italy. *Sci. Rep.* 8 (8), 1–16. doi:10.1038/s41598-018-34444-1

Doglioni, C., Moretti, I., and Roure, F. (1991). Basal Lithospheric Detachment, Eastward Mantle Flow and Mediterranean Geodynamics: A Discussion. *J. Geodynamics* 13, 47–65. doi:10.1016/0264-3707(91)90029-E

Faivre, S., and Reiffsteck, P. (2016). From Doline Distribution to Tectonics Movements Example of the Velebit Mountain Range, Croatia. *Ac* 31. doi:10.3986/ac.v31i3.384

Faivre, S., and Reiffsteck, P. (1999). Spatial distribution of dolines as an indicator of recent deformations on the Velebit mountain range (Croatia)/La répartition spatiale des dolines comme indicateur de contraintes tectoniques. Montagne de Velebit (Croatie). *morfo* 5, 129–142. doi:10.3406/morfo.1999.983

Fronzi, D., Mirabella, F., Cardellini, C., Caliro, S., Palpacelli, S., Cambi, C., et al. (2021). The Role of Faults in Groundwater Circulation before and after Seismic Events: Insights from Tracers, Water Isotopes and Geochemistry. *Water* 13, 1499. doi:10.3390/W13111499

Galadini, F., and Galli, P. (2000). Active Tectonics in the Central Appennines (Italy) - Input Data for Seismic hazard Assessment. *Nat. Hazards* 22, 225–268. doi:10.1023/A:1008149531980

Galli, P., Galadini, F., and Pantosti, D. (2008). Twenty Years of Paleoseismology in Italy. *Earth-Science Rev.* 88, 89–117. doi:10.1016/j.earscirev.2008.01.001

Gudmundsson, A. (2000). Active Fault Zones and Groundwater Flow. *Geophys. Res. Lett.* 27, 2993–2996. doi:10.1029/1999GL011266

Herold, T., Jordan, P., and Zwalhen, F. (2000). The Influence of Tectonic Structures on Karst Flow Patterns in Karstified Limestones and Aquitards in the Jura Mountains, Switzerland. *Eclogae Geol. Helv.* 93, 349–362.

Ingebritsen, S. E., and Manga, M. (2019). Earthquake Hydrogeology. *Water Resour. Res.* 55, 5212–5216. doi:10.1029/2019WR025341

ISRM (1978). Suggested Methods for the Quantitative Description of Discontinuities in Rock Masses. *Int. J. Rock Mech. Min. Sci. Geomech. Abstr.* 15, 319–368. doi:10.1016/0148-9062(78)91472-9

Karfakis, J., and Loupasakis, C. (2006). "Geotechnical Characteristics of the Formation of "Tourkovounia" Limestones and Their Influence on Urban Construction-City of Athens, Greece," in *IAEG 2006* (Nottingham, United Kingdom: Geological Society of London).

Malinverno, A., and Ryan, W. B. F. (1986). Extension in the Tyrrhenian Sea and Shortening in the Apennines as Result of Arc Migration Driven by Sinking of the Lithosphere. *Tectonics* 5, 227–245. doi:10.1029/TC005i002p00227

Mastrorillo, L., Saroli, M., Viaroli, S., Banzato, F., Valigi, D., and Petitta, M. (2020). Sustained post-seismic Effects on Groundwater Flow in Fractured Carbonate Aquifers in Central Italy. *Hydrological Process.* 34, 1167–1181. doi:10.1002/HYP.13662

Montone, P., and Salvini, F. (1991). Evidence of Strike-Slip Tectonics in the Apennine Chain Near Tagliacozzo (L'Aquila), Abruzzi, central Italy. *Boll. Della Soc. Geol. Ital.* 110, 707–716.

Montone, P., and Salvini, F. (1993). Geologia strutturale dell'area tra Colli di Monte Bove (Carsoli) e Tagliacozzo, Abruzzo, Italia Centrale. *Geol. Rom.* 29, 15–29.

Mostardini, F., and Merlini, S. (1986). Appennino centro meridionale: sezioni geologiche e proposta di modello strutturale. *Mem. Della Soc. Geol. Ital.* 35, 177–202.

Nisio, S., and Scapola, F. (2010). "I Sinkholes Nel Frusinate," in *Atti 2° Workshop Internazionale "I Sinkholes. Gli Sprofondamenti Catastrofici Nell'ambiente Naturale Ed in Quello Antropizzato"* (Roma: ISPRA), 329–348.

Öztürk, M. Z., Şener, M. F., Şener, M., and Şimşek, M. (2018). Structural Controls on Distribution of Dolines on Mount Anamas (Taurus Mountains, Turkey). *Geomorphology* 317, 107–116. doi:10.1016/j.geomorph.2018.05.023

Pardo-Igúzquiza, E., Dowd, P. A., and Telbisz, T. (2020). On the Size-Distribution of Solution Dolines in Carbonate Karst: Lognormal or Power Model? *Geomorphology* 351, 106972. doi:10.1016/J.GEOMORPH.2019.106972

Patacca, E., Sartori, R., and Scandone, P. (1990). Tyrrhenian basin and Apenninic Arcs: Kinematic Relations since Late Tortonian Times. *Mem. Della Soc. Geol. Ital.* 45, 425–451.

QGIS Development Team (2022). QGIS Geographic Information System Ver. 3.22. Available at: http://qgis.osgeo.org.

Rosen, M. R., Binda, G., Archer, C., Pozzi, A., Michetti, A. M., and Noble, P. J. (2018). Mechanisms of Earthquake-Induced Chemical and Fluid Transport to Carbonate Groundwater Springs after Earthquakes. *Water Resour. Res.* 54, 5225–5244. doi:10.1029/2017WR022097

Rovida, A., Locati, M., Camassi, R., Lolli, B., Gasperini, P., and Antonucci, A. (2021). Catalogo Parametrico dei Terremoti Italiani (CPTI15), versione 3.0. *Ist. Naz. di Geofis. e Vulcanol.* doi:10.13127/CPTI/CPTI15.3

Salvati, R., and Sasowsky, I. D. (2002). Development of Collapse Sinkholes in Areas of Groundwater Discharge. *J. Hydrol.* 264, 1–11. doi:10.1016/S0022-1694(02)00062-8

Santangelo, N., and Santo, A. (1991). "Endokarstic Evolution of Carbonatic Massifs in Campania (Southern Italy): Geological and Geomorphological Implications," in *Proceedings Ofthe International Conference on Environmental Changes in Karst Areas -I* (Italy: G.U.- U.I.S).

Saroli, M., Biasini, A., Cavinato, G. P., and Di Luzio, E. (2003). Geological Setting of the Southern Sector of the Roveto Valley (Central Apennines, Italy). *Boll. Della Soc. Geol. Ital.* 122, 467–481.

Saroli, M., Moro, M., Cinti, F. R., and Montone, P. (2006). La faglia Val Roveto-Atina (Appennino Centrale): evidenze di attività tettonica Quaternaria. *GNGTS*, 89–90.

Saroli, M., Moro, M., Florindo, F., Lancia, M., Lurcock, P. C., and Dinarès-Turell, J. (2015). Paleomagnetic Dating of Tectonically Influenced Plio-Quaternary Fan-System Deposits from the Apennines (Italy). *Ann. Geophys.* 58, 1–5. doi:10.4401/ag-6740

Saroli, M., Moro, M., Gori, S., Falcucci, E., and Salvatore, M. C. (2012). "Tettonica, idrogeologia e carsismo: un nuovo approccio multidisciplinare per lo studio della tettonica attiva. L'esempio della faglia di Posta Fibreno (Marsica occidentale Lazio Meridionale)," in *IV Congresso AIGA* (Perugia: EngHydroEnv Geology), 215–216. doi:10.1474/EHEGeology.2012-14.B.160

Scrocca, D., and Tozzi, M. (1999). Tettogenesi mio-pliocenica dell'Appennino molisano. *Boll. Soc. Geol. Ital.* 118, 255–286.

Šegina, E., Benac, Č., Rubinić, J., and Knez, M. (2018). Morphometric Analyses of Dolines - the Problem of Delineation and Calculation of Basic Parameters. *Ac* 47, 23–33. doi:10.3986/AC.V47I1.4941

Serafini, S., and Vittori, E. (1988). Caratteri tettonici desunti da dati mesostrutturali nell'area compresa tra Sora e le gole di Atina (Lazio Meridionale). *Mem. Della Soc. Geol. Ital.* 41, 1191–1199.

Shanov, S., and Kostov, K. (2015). *Dynamic Tectonics and Karst*. Berlin, Heidelberg: Springer Berlin Heidelberg. doi:10.1007/978-3-662-43992-0

Stucchi, M., Meletti, C., Montaldo, V., Akinci, A., Faccioli, E., Gasperini, P., et al. (2004). *Pericolosità sismica di riferimento per il territorio nazionale MPS04*. doi:10.13127/sh/mps04/ag

Thery, J., Pubellier, M., Thery, B., Butterlin, J., Blondeau, A., and Adams, C. (1999). Importance of Active Tectonics during Karst Formation. A Middle Eocene to Pleistocene Example of the Lina Moutains (Irian Jaya, Indonesia). *Geodinamica Acta* 12, 213–221. doi:10.1016/S0985-3111(00)88660-X

Tiberti, M. M., Orlando, L., Di Bucci, D., Bernabini, M., and Parotto, M. (2005). Regional Gravity Anomaly Map and Crustal Model of the Central-Southern Apennines (Italy). *J. Geodynamics* 40, 73–91. doi:10.1016/J.JOG.2005.07.014

Verbovšek, T., and Gabor, L. (2019). Morphometric Properties of Dolines in Matarsko Podolje, SW Slovenia. *Environ. Earth Sci.* 78, 1–16. doi:10.1007/S12665-019-8398-6/FIGURES/12

Conflict of Interest: The authors declare that the research was conducted in the absence of any commercial or financial relationships that could be construed as a potential conflict of interest.

Publisher's Note: All claims expressed in this article are solely those of the authors and do not necessarily represent those of their affiliated organizations, or those of the publisher, the editors and the reviewers. Any product that may be evaluated in this article, or claim that may be made by its manufacturer, is not guaranteed or endorsed by the publisher.